

Tensile yield parameters for poly(vinyl chloride) blends with a methyl methacrylate/ethyl acrylate copolymer

S. Havriliak Jr, S. E. Slavin and T. J. Shortridge

Research Division, Rohm and Haas Co., Bristol Research Park, Bristol, PA 19006, USA

(Received 11 December 1989; revised 10 March 1990; accepted 23 March 1990)

Tensile yield measurements were made on blends of poly(vinyl chloride) (PVC) with a methyl methacrylate/ethyl acrylate 90/10 copolymer (CP-A) covering a blend range of 0 to 50 wt% CP-A, a temperature range of -50 to 50°C and a strain-rate range of 10^{-3} to 10^0 s^{-1} . Increasing CP-A level in PVC has the same effect on the brittle-to-ductile transition as does decreasing temperature or increasing strain rate in neat PVC. The maximum stresses observed for these blends tend to be independent of CP-A level over the low-concentration range, i.e. $<25 \text{ wt}\%$, but they do decrease over the 50 wt% range. The tensile yield stress variation with temperature and strain rate was represented in terms of the Ree-Eyring-Roetling rate model. This model represents the experimental data within experimental error. The tensile yield beta process parameters were compared to those determined from viscoelastic measurements on these same blends. The activation energies were found to be the same for the viscoelastic and tensile yield measurements, while the entropies of activation were found to be proportional.

(Keywords: poly(vinyl chloride); polymer blends; tensile yield; poly(methyl methacrylate))

INTRODUCTION

The Ree-Eyring-Roetling¹⁻⁴ model for tensile yielding is based on polymer segments jumping over energy barriers to relieve the applied stress. In some cases two barriers must be postulated to account for the experimental results. In this model the yield stress dependence on strain rate and temperature is represented in terms of polymer segment jumping probabilities and its dependence on such parameters as activation entropy or energy. The tensile yield behaviour of poly(vinyl chloride) (PVC) was first studied and treated in terms of this model by Bauwens-Crowet *et al.*⁵. They found that the tensile yield variation with strain rate and temperature could be represented in terms of this model, and determined the activation energies for the slow (alpha) and fast (beta) processes.

A correspondence between the activation energies determined from dielectric as well as viscoelastic relaxation measurements with those determined from the Ree-Eyring-Roetling representation of tensile yield dependence on strain rate and temperature was recently reported^{6,7} for a small number of polymers. The beta process of PVC was also included in those studies. In addition, the equivalence of dielectric and viscoelastic beta process dynamic parameters in PVC was described. A similar study for the dynamic beta process parameters for polycarbonate (PC)⁸ was also reported.

Previous studies reported on the dynamics of the viscoelastic beta process in neat PVC⁹. The effects of molecular weight¹⁰ and impact modifier level on these dynamic parameters were also reported^{11,12}. Modifier was found to enhance the PVC beta process by increasing its magnitude, decreasing its relaxation time and narrowing its relaxation time distribution so that the molecular responses are concentrated in the strain-rate range of 10^0

to 10^6 s^{-1} . The effect of molecular weight was found to be small. The effect of a methyl methacrylate/ethyl acrylate copolymer (CP-A), thought to be compatible with PVC, on the beta process parameters of PVC was also reported¹³. Increasing the CP-A level from 0 to 25 wt% not only had the effect of diluting the beta process in PVC but was also found to interfere with the dynamics of the process. In other words, increasing CP-A level tended to broaden the relaxation time distribution as well as increase the average time of the process. The results are similar to what might have been qualitatively predicted from the Perchak¹⁴ or Mansfield¹⁵ models for polymer dynamics, since both these models interpret polymer dynamics in terms of an interaction of a chain segment with its environment.

In this work we report the results of a tensile yield study on the same PVC/CP-A blends as were used in the viscoelastic study¹³. It is the objective of this study to determine how the dynamic changes observed in a viscoelastic study¹³ are related to the tensile yield properties of the blend.

EXPERIMENTAL METHODS

Materials and test specimens

Preparation of the materials and powder formulations used in this study have been described before¹³ in a viscoelastic study of the beta process. Briefly, CP-A is a methyl methacrylate/ethyl acrylate 90/10 copolymer prepared by emulsion polymerization and has a weight-average molecular weight of 1.8×10^6 . The PVC used in this work is a commercial product with a weight-average molecular weight of 1.0×10^5 (K58 value). Test specimens were cut from plaques prepared by first milling powder blends then compression moulding the fused

mass to form plaques 8 inch \times 10 inch \times 0.125 inch (\sim 200 mm \times 250 mm \times 3 mm). The powder blends were lightly lubricated and stabilized. The contents of CP-A studied were 0, 2, 5, 10, 15, 25 and 50 wt%. All levels were clear, indicating compatibility, except for the 50 wt%. Plaques at this level were slightly cloudy, indicating incomplete compatibilization of CP-A with PVC. For this reason higher CP-A levels were not studied. Reference to the specific levels for the remainder of this work is in terms of weight per cent of CP-A in PVC.

Tensile yield measurements

All test specimens were saw-cut from the compression-moulded plaques and shaped into ASTM type 5 tensile bars using a Tensicut router and appropriate fixture. Preliminary experimentation with strip samples proved that the yield results were unreliable because of the high incidence of breaks within the pneumatic grips. Conversion to the microtensile shape eliminated this problem and also resulted in a 5–7% increase in the observed yield stresses. These higher stresses are likely to be associated with the removal of extrusive grip forces from the gauge section.

A Mitutoyo digital micrometer was employed to measure the initial cross-sectional dimensions of each sample to the nearest ten-thousandth of an inch (\sim 2.5 μ m). Owing to the inherent difficulty associated with monitoring the sample cross-section during elongation, it is these initial dimensions that are used to calculate the reported yield stresses from the maximum loads. Although this technique of calculating the yield stress is in accordance with ASTM test method D 638, it is recognized that the actual stresses are somewhat higher than reported owing to the reduction in cross-section that accompanies specimen elongation.

All tensile yield measurements were performed using an Instron model 4202 universal tester with computer control and data acquisition. Experiments were performed at constant crosshead rates, which spanned the full range available on the instrument. Samples were conditioned in the electrically heated and liquid-nitrogen-cooled environmental chamber at the desired test temperature for a minimum of 30 min and allowed to reside in the grips for 10 min after insertion. The ambient temperature was maintained at the desired level \pm 0.5°C by a controller with a thermocouple sensor and monitored using a standard laboratory thermometer.

Reported strain rates were determined using the initial gauge length of the specimens, without correction for the decrease associated with sample extension at a constant crosshead speed. A high-speed digital storage oscilloscope was employed to monitor the load cell output as a back-up for the computerized data acquisition system. Maximum load readings from the computer and oscilloscope were in excellent agreement up to crosshead rates of one inch per minute (\sim 0.4 mm s⁻¹); deviations were observed at higher rates. These deviations result from the fact that the maximum computer sampling rate of 20 points per second is insufficient for the higher rates of loading and rapid yielding encountered during this experiment. The plots consisted of straight-line segments connecting the points and suggested that the actual maximum loads were occurring in the interval between data points. At crosshead rates in excess of one inch per minute, the probability of sampling at precisely the

moment of peak loading is quite low, and the variation in the maximum loads observed with standard materials supports this conclusion. For these reasons, reported stress values at high crosshead rates were derived using load readings obtained from the oscilloscope.

Tensile yield measurements were made at -50 , -25 , 0 and 23°C for 0 to 25 wt% CP-A samples covering the strain rates indicated above. The 50 wt% samples broke at any strain rate for the lowest two temperatures. For this reason, the temperature range was extended to 35 and 50°C for the 50 wt% samples. A limited amount of data are available for the CP-A.

Numerical analysis

Experimental data were assembled and analysed in a SAS¹⁶ data set. SAS is a user-friendly, versatile statistical software package. The regressions were carried out with SAS's PROC NLIN using their DUD method. All statistical results reported here were derived from that software routine. Calculations were performed on an IBM mainframe model 3090.

D.s.c. measurements

D.s.c. measurements were made on 20 mg (approximate) test specimens in a Perkin Elmer DSC-7 differential scanning calorimeter at a heating rate of 20°C min⁻¹. D.s.c. glass temperatures were calculated using their software.

RESULTS

D.s.c. measurements

A plot of the d.s.c. T_g with CP-A level is given in Figure 1. The full line was determined from a least-squares fit of the data. The broken line was determined from the values of the neat components and assuming that intermediate values were related to linear weight per cent CP-A. The two lines are, within experimental error, the same.

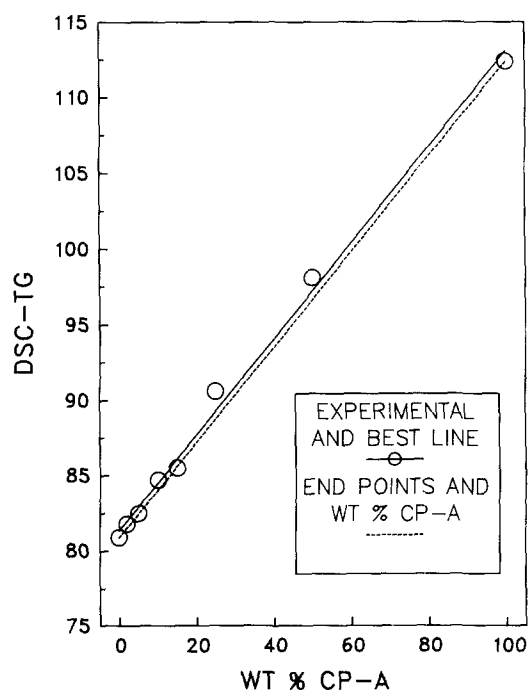


Figure 1 A plot of the d.s.c. T_g (°C) with weight per cent CP-A. The significance of the lines is defined in the legend and discussed in the text

Table 1 Statistical parameters describing the reproducibility of the tensile yield measurement and the quality of the fit in terms of the Ree–Eyring–Roetling model

Parameter ^a	0 wt% CP-A	2 wt% CP-A	5 wt% CP-A	10 wt% CP-A	15 wt% CP-A	25 wt% CP-A	50 wt% CP-A
E-VAR	153.8	130.6	217.8	230.2	1412	347.2	415.6
E-S.D.	12.37	11.46	14.76	15.19	37.68	18.63	22.07
MEAN	933	932	930	949	1017	981	814
E-C.V.	1.3	1.2	1.6	1.6	3.71	1.9	2.71
P-VAR	349	728	402	617	635	541	485
P-C.V.	2.0	2.8	2.2	2.6	2.5	2.4	2.7
N-OBS.	59	53	53	53	58	54	52

^aSee text for definition of statistical terms**Table 2** Conditions under which the yield stress was observed to be a maximum

Parameter ^a	0 wt% CP-A	2 wt% CP-A	5 wt% CP-A	10 wt% CP-A	15 wt% CP-A	25 wt% CP-A	50 wt% CP-A
Stress (psi)	1420	1624	1469	1335	1483	1357	998
Strain rate (S ⁻¹)	4	20	20	1	10	40	1
Temperature (°C)	-50	-50	-50	-50	-50	-50	0

^aSee text for details

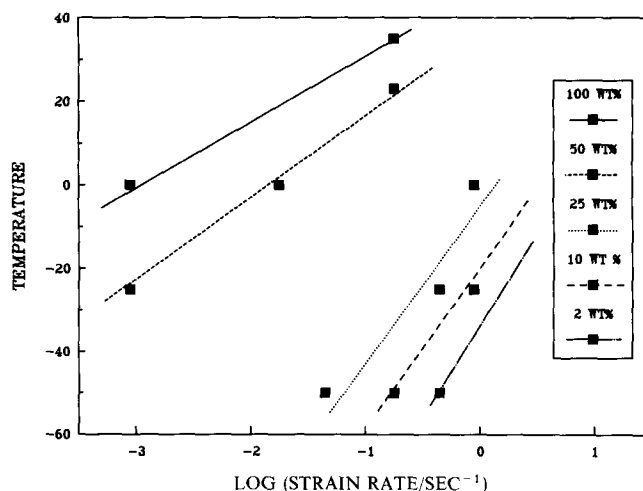
Replication studies

About 90% of the experimental settings were replicated so that variances¹⁷ could be calculated from the corrected sums of squares over the entire strain-rate, temperature and CP-A level range. The experimental variances (E-VAR) are given in *Table 1* for the various concentrations of copolymer CP-A. There is a tendency for the E-VAR to increase with CP-A level. Square root of E-VAR leads to the standard deviation (E-S.D.), which also tends to increase with CP-A level. The row listed as MEAN is the average value of the yield stress over the experimental range and at constant CP-A level. The MEAN is essentially independent of CP-A level, suggesting that the data are balanced and that magnitude of the variable is not a problem when comparisons are made. The ratio of E-S.D. to MEAN $\times 100$ is the experimental coefficient of variation (E-C.V.) in per cent. The experimental coefficient of variation ranged from 1.3 to 3.7% over the composition range.

Preliminary view of the data

A number of useful results can be extracted from the data. In *Table 2* we have listed the conditions under which the maximum yield stress was observed. For CP-A levels of 0 to 25 wt% the stress is constant at about 1480 kg cm⁻². At 50 wt% CP-A level the stress falls to a much lower value, supporting the observation that CP-A at this level might not be compatible.

A failure envelope can be constructed from the data because of the experimental design. This design consisted of the same four temperatures and the same eight strain rates for all the compositions. A temperature–strain rate array of the data for each composition quickly showed the brittle-to-ductile transition. We define the failure condition as the strain rate at a given temperature at which the specimen breaks instead of yielding. The failure condition was replicated at the next higher strain rate but never at the second highest since each experimental condition was repeated. This boundary also defines the brittle-to-ductile transition. These failure

**Figure 2** Failure envelope for PVC/CP-A blends. The boundaries shown here separate the ductile from the non-ductile behaviour of the blends

conditions can be plotted for a number of blends to define a failure envelope dependence on weight per cent CP-A. These plots are given in *Figure 2* for some of the blends. Failure was not observed for the 0 wt% blend in this region. The 5 and 15 wt% levels were deleted because they overlap the 10 wt%. Line segments have been drawn through the points to show their approximate behaviour.

Results of time–temperature shifting

Plots of the yield stresses with log strain rates for the four temperatures are given in *Figure 3* for neat PVC. The results of shifting the data are given in *Figure 4* for these temperatures. Shifting was readily accomplished and the individual temperatures are labelled in the legend. Mean values of the yield stresses were used in all cases. The results of shifting all of the data are given in *Figure 5* and the CP-A levels are indicated in the legend. Plots of the log shift factors with temperature are given in *Figure 6*.

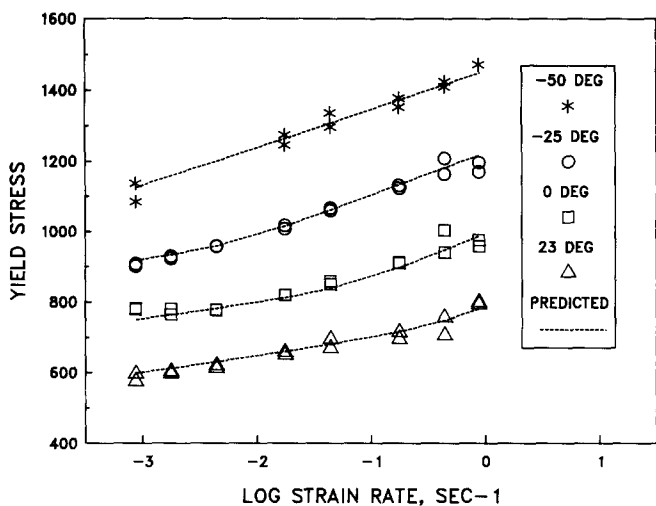


Figure 3 Variation of tensile yield (in kg cm⁻²) for PVC as a function of log(strain rate, in s⁻¹) at the four temperatures of measurement (in °C). The experimental quantities are represented by the symbols defined in the legend while the broken curves represent calculated values

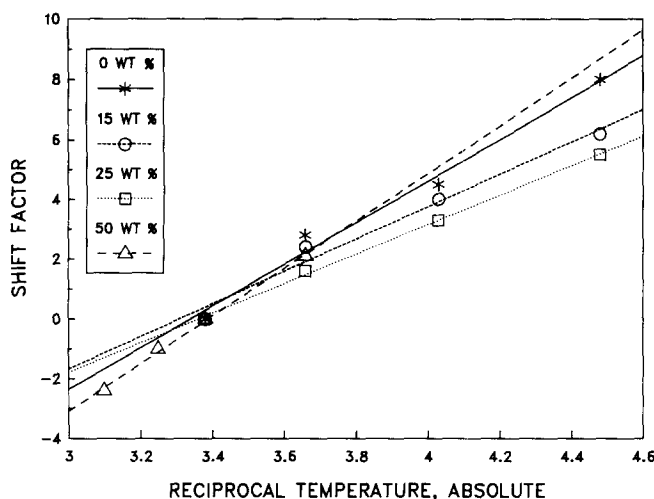


Figure 6 Shift factors for the various CP-A levels plotted against reciprocal absolute temperature

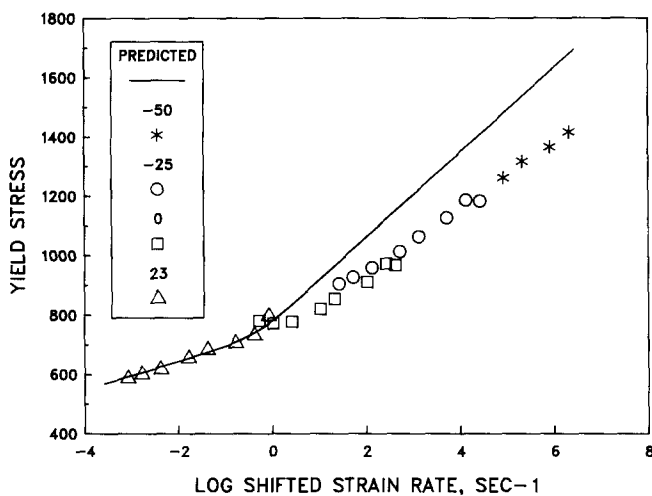


Figure 4 Results of time-temperature shifting the experimental data shown in Figure 3. The temperatures are defined in the legend. The full curve represents calculated values over the entire shifted strain-rate range for 0 wt% CP-A and 23°C

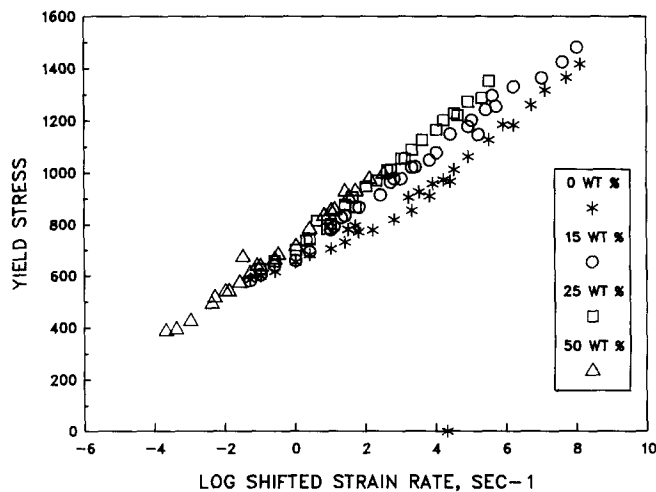


Figure 5 Results of shifting all of the CP-A levels. The legend identifies the various levels

Regression results

The Ree-Eyring-Roetling (RER) model for the yield stress dependence on strain rate and temperature, assuming two processes, is:

$$\sigma_0/T = A_\alpha[\ln(2C_\alpha\dot{\epsilon}) + (Q_\alpha/RT)] + A_\beta \sinh^{-1}[C_\beta\dot{\epsilon} \exp(Q_\beta/RT)] \quad (1)$$

In this expression σ_0 is the yield stress, $\ln \dot{\epsilon}$ is the strain rate, R is the gas constant and T is the absolute temperature. The subscripts α and β represent the alpha and beta processes, i.e. slow and fast processes; the significance of the remaining parameters is given in refs. 1-4.

Initial attempts to regress the tensile yield data by allowing C_α and C_β to be variables of the regression along with the parameters A_α , Q_α , A_β and Q_β using SAS PROC NLIN failed. The failure was traced to the observation that these two parameters form a very shallow minimum and that any value in the range of the exponent is a suitable choice. This problem was resolved by applying a stepwise procedure to the regression. In this technique, values for the two C s were fixed to the values listed in ref. 12, while allowing the other four parameters to be variables of the regression. Once these four parameters were determined, they were fixed and the two C s were allowed to vary. Finally the two C s were fixed and the four parameters were redetermined. The results for the stepwise regression are given in Table 3 for PVC and its six blends.

A plot of the predicted yield stress as a function of strain rate and temperature is plotted in Figure 3 for the 0 wt% CP-A. The agreement with the experimental results discussed previously appears to be excellent. This is a superficial comparison of experimental versus predicted results; there are better methods of comparison. If we define the residuals to be the difference between experimental and predicted values and then take the ratio of the residual to the MEAN $\times 100$ we have the residual in per cent. A plot of residual (%) versus $\log \dot{\epsilon}$ for the various temperatures is given in Figure 7 along with the experimental confidence limits, i.e. E-C.V. Inspection of the data in Figure 3 does not reveal any systematic trends and most of the data are within the experimental confidence limits. Specifically 52% of the residuals are

Table 3 Parameter estimates and their confidence intervals for representing the tensile yield properties of PVC/CP-A blends in terms of the Ree–Eyring–Roetling model

Parameter ^a	0 wt% CP-A	2 wt% CP-A	5 wt% CP-A	10 wt% CP-A	15 wt% CP-A	25 wt% CP-A	50 wt% CP-A
Alpha process parameters							
$A_\alpha \times 10^4$	7.3	7.60	6.99	6.55	6.25	6.53	8.5
S.D.	0.2	0.26	0.30	0.28	0.29	0.23	0.4
Q_α	71.8	70.8	72.8	73.2	73.9	73.9	69.5
S.D.	0.5	0.7	0.7	0.4	0.9	0.8	0.4
$C_\alpha \times 10^{38}$	2.1	0.76	0.73	0.76	0.71	0.70	0.69
S.D.	0.4	0.20	0.22	0.26	0.33	0.38	0.17
Beta process parameters							
$A_\beta \times 10^4$	14.2	21.6	9.6	11.7	13.7	12.0	7.6
S.D.	0.09	0.2	1.1	0.3	0.9	0.1	0.8
Q_β	12.3	12.0	13.6	13.6	14.1	15.0	16
S.D.	0.2	0.2	0.3	0.4	0.2	0.3	0.4
$C_\beta \times 10^{38}$	10.7	4.28	4.5	4.28	4.0	4.5	4.6
S.D.	1.7	0.73	1.4	0.26	1.0	1.5	1.5

^aSee text for details

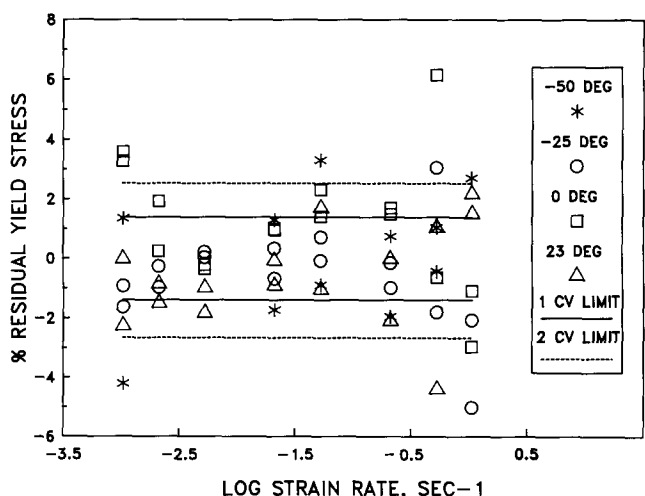


Figure 7 Percent residual stress for PVC as a function of log(strain rate, in s^{-1}) at the four temperatures (in $^{\circ}C$) defined in the legend

within $2 \times E-C.V.$ and 84% are within $4 \times E-C.V.$ The residuals can be squared, then summed and divided by the degrees of freedom to yield the predicted variance, P-VAR listed in Table 1. Taking the ratio of P-VAR to the MEAN and multiplying by 100 yields P-C.V., also listed in Table 1. P-C.V. is independent of CP-A level and is less than $2 \times E-S.D.$ In other words, the residuals of the regression have been brought within a factor of 2 of the experimental variability.

Another way to examine the nature of the residuals is with a bar chart or population distribution chart. In this plot, the population in a given range of P-C.V. is plotted against P-C.V. Since P-C.V. is about 2 we have taken the range to be 0.5. The number of residuals in any range, say -2.0 to -2.29 , is plotted against P-C.V. The results are shown in Figure 8 for all of the blends. In addition, a normal distribution curve is included. The normal distribution curve is calculated for the mean of P-C.V.s (2.46) listed in Table 1. The normal curve was then scaled

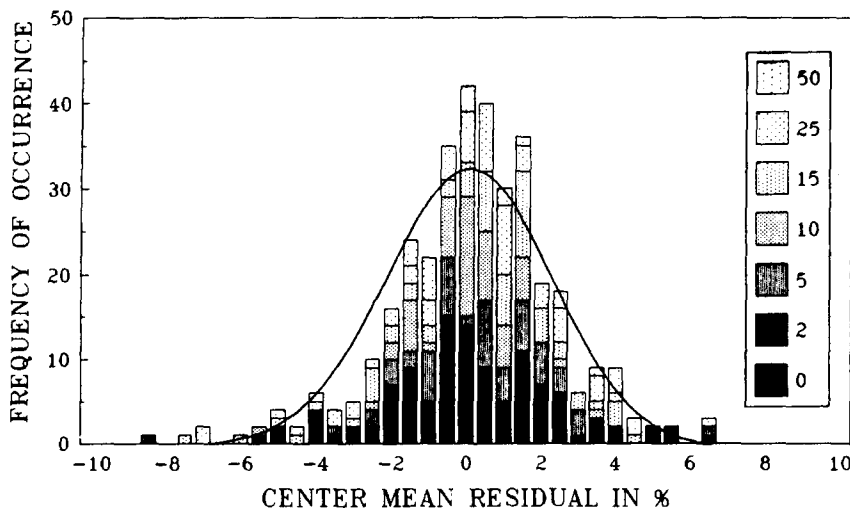


Figure 8 Frequency distribution plot of the residuals (expressed as %) for the various CP-A levels defined in the legend

so that the integrated area under the normal curve is equal to the integrated area in the total bar graph for all the blends. A number of observations can be made from *Figure 8*. First, the experimental distribution curve is slightly skewed; the peak is about +0.5 to +1.0%, which is less than one-half of a P-C.V. Secondly, there is no clear trend with CP-A level. In other words, increasing CP-A level does not change either the size of P-C.V. or its bias. The shape of the distribution is similar to that reported previously even though E-C.V. has been reduced sixfold.

DISCUSSION

D.s.c. results show the polymers are compatible over the composition range studied even though a slight haze was observed at 50 wt%. The full line in *Figure 1* represents the result of a least-squares fit of the data. The broken line represents the results of calculating the intermediate glass temperatures by assuming weight per cent additivity and the experimental values for the pure components. The agreement between the two methods is the same, within experimental error.

In the discussion that follows, stresses are calculated from loads with respect to the original specimen dimensions, i.e. these are engineering stresses and not true stresses. Although a precise discussion should be based on true stress and not on engineering stress, a number of important points can nevertheless be made in terms of engineering stresses.

The results shown in *Figure 2*, free from any model assumptions or curve-fitting errors, indicate that increasing CP-A level either increases the temperature or reduces the strain rate of the brittle-to-ductile transition. It should be restated that neat PVC did not break without first yielding in this experimental range. In other words the brittle-to-ductile transition is below and to the right of the data in *Figure 2*. In addition, at least over the 0 to 25 wt% range, the maximum stresses observed are constant. Although the exact position of the brittle-to-ductile transition for the 50 and 100 wt% may be influenced by stress lowering, they are, however, positioned in a way that is consistent with the lower concentrations of CP-A.

The results shown in *Figure 3* can be qualitatively interpreted in terms of Perchak's or Mansfield's models. In either model, addition of a stiff polymer chain to the PVC system on the molecular level is expected to interfere with the dynamics of the PVC beta process. We can assume that CP-A is a stiff polymer chain because its beta process is to the low-frequency and/or high-temperature side of the beta process in PVC¹³. Furthermore, the real compliance under any experimental conditions studied was always lower for CP-A. The remaining discussion is an attempt to quantify these molecular interactions.

Time-temperature shifting of the data appears to lead to reasonable results, though somewhat different from those obtained from the RER model shown in *Figure 4*. The reason for this difference is that the shifting method assumes a single process while the RER method assumes two processes. In either case, the results in *Figure 5* clearly show that addition of CP-A to PVC increases the yield stress at any of the strain rates studied.

There are two important differences in the data analysis between the previous viscoelastic study¹³ and the present

tensile yield study. First, the contribution of the alpha process to the beta process region is cleanly separated in the viscoelastic case. Secondly, the experimental complex compliance of CP-A times its weight fraction could be subtracted from the complex compliance of the blend at any temperature or frequency. The resulting difference could then be analysed and the parameters compared to neat PVC. The dependence of the parameters on weight fraction PVC could then be determined. In the present study these conditions do not exist, thereby confounding the effects of overlapping processes as well as contributions from CP-A to the yield stress. On the other hand, if this assumption is invalid, then one would see a significant increase of residuals with CP-A level, which is not observed. Comparison of statistical parameters such as P-C.V. does not indicate a significant breakdown of the RER model with CP-A level for these blends, so that equation (1) is applicable.

Inspection of the equation (1) parameters given in *Table 3* shows that a number of small changes may take place upon the addition of CP-A. Some of these changes are several times larger than the confidence intervals for the parameter estimates and should be noted. Q_β correlates very strongly (r -square = 0.97, see ref. 16) but has a very small effect with linear weight per cent CP-A. Modest correlations can be noted for C_α (r -square = 0.6) and C_β (r -square = 0.6). The parameter A_α , which has a poor linear correlation with CP-A level (r -square = 0.4), appears to have a minimum at 15 wt% while Q_α appears to have a maximum in the same CP-A range. The changes just noted are small and difficult to interpret.

The effect of these small parameter changes can be seen by estimating the yield stress dependence of strain rate at 0°C for a number of blends. The results are shown in *Figure 9* for CP-A 0, 25 and 50 wt% blends and a log strain rate range of -4 to 3 s^{-1} . Strain rates are deleted from the graph when they lead to stresses in excess of

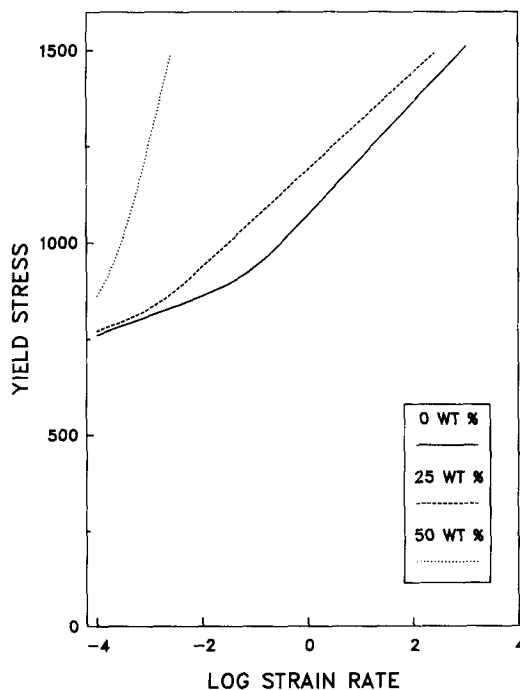


Figure 9 Plot of the total yield stress with strain rate at room temperature for the three polymer blends listed in the legend

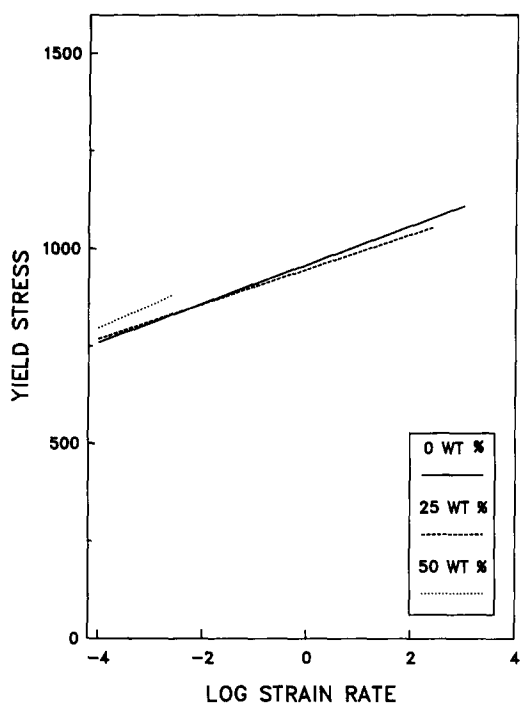


Figure 10 Plot of the alpha process contribution to the yield stress with strain rate at room temperature for the three polymer blends listed in the legend

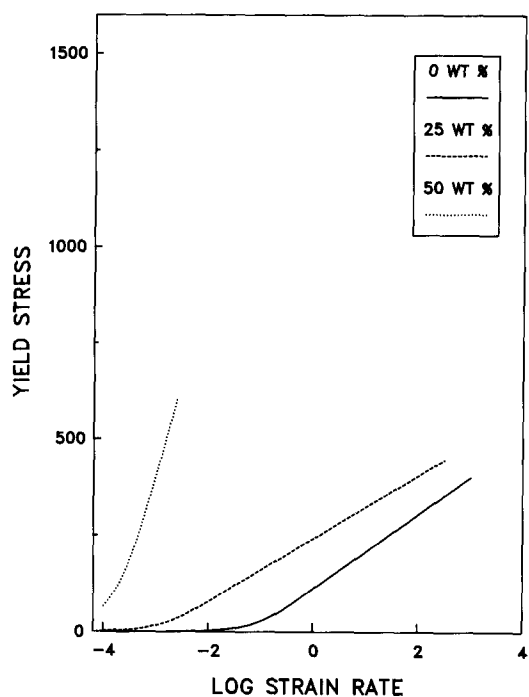


Figure 11 Plot of the beta process contribution to the yield stress with strain rate at room temperature for the three polymer blends listed in the legend

1500 kg cm⁻², the maximum experimental value observed. For cases when the stress was below this limit, the data were extrapolated beyond the experimental range. The yield stresses for 50 wt% exhibit a significant increase over the other two compositions. In Figure 10 we have plotted the alpha process contribution to the total yield stress. The behaviour observed in this figure suggests that it is not the alpha process that changes significantly with weight per cent CP-A. A plot of the yield stress contribution from the beta process is shown in Figure 11. It is apparent from these results that the sudden rise is entirely due to changes in the beta process parameters with CP-A level. We can conclude from these results that it is the dynamics of the beta process that is important at high strain rates and at room temperature.

Perhaps the best interpretation of the tensile yield parameters is a comparison with their viscoelastic counterparts¹⁵. In that work the temperature dependence of the viscoelastic relaxation time was assumed to be given by an Arrhenius expression of the form:

$$\ln f_0 = I_3 + C_3(AK - AK_0) \quad (2)$$

(Note: *A* has replaced *R* in the previous work to avoid confusion with the gas constant *R* to be used below.) In this expression *f*₀ is the relaxation frequency in radian cycles s⁻¹, and *I*₃ and *C*₃ are results (parameters) of the regression, which are listed in Table 4. *AK* is 1000/*K* and *K* is temperature in degrees kelvin. *AK*₀ is the reciprocal of the reference temperature (*T*₀ = -50°C), chosen to centre the relaxation process about *T* - *T*₀ = 0. In other words *T*₀ was chosen to balance the data set with respect to temperature dependences. For the present purpose we take *AK*₀ = 4.484. Equation (2) can be expanded to read:

$$\ln f_0 = I_3 - (AK_0)C_3 + C_3/K \quad (3)$$

If we multiply the numerator and denominator of the last term on the RHS by *R*, the gas constant, and identify $\Delta E = -RC_3$ and $\Delta S = R[I_3 - (AK_0)C_3]$ this leads to:

$$\ln f_0 = \frac{\Delta S}{R} - \frac{\Delta E}{RK} \quad (4)$$

In the following equations we make the temporary substitution that *T* = *K*. Taking antilogarithms of both sides leads to:

$$f_0 = \exp(\Delta S/R) \exp(-\Delta E/RT) \quad (5)$$

$$f_0 = \exp[-(\Delta E - T\Delta S)/RT] \quad (6)$$

where *T*, only in equations (5) and (6), is *T* = *K* in degrees kelvin. Equation (6) gives the (jumping) frequency in terms of the familiar free energy of activation and refers to the viscoelastic process. The first product on the RHS

Table 4 Slopes and intercepts for the rate plot of the viscoelastic beta relaxation process in PVC and its blends with CP-A

Parameter ^a	0 wt% CP-A	2 wt% CP-A	5 wt% CP-A	10 wt% CP-A	15 wt% CP-A	25 wt% CP-A
<i>I</i> ₃	-6.4	-6.6	-7.5	-6.0	-6.5	-6.0
<i>C</i> ₃	-2.7	-1.56	-2.77	-2.97	-4.87	-1.76
<i>AK</i> ₀	4.484	4.484	4.484	4.484	4.484	4.484
ΔE	12.7	13.1	14.9	11.9	12.9	11.9
ΔS	22.43	24.18	26.62	20.65	20.94	21.63
ΔS_n	10.48	11.3	12.4	9.65	9.79	10.13

^aSee text for details

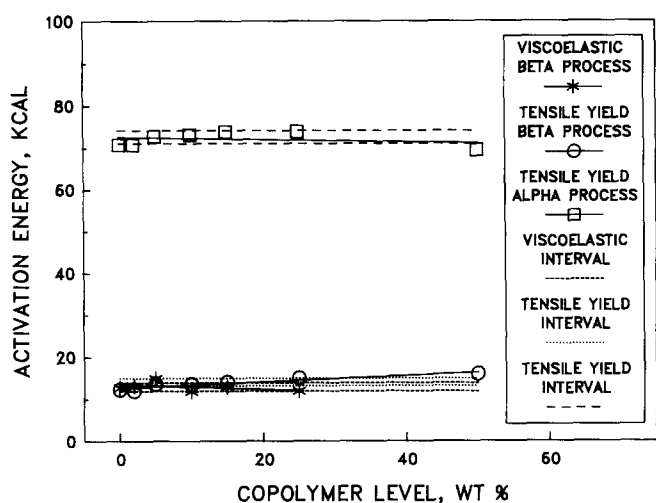


Figure 12 Activation energy (in kcal mol⁻¹) as a function of CP-A level (in wt%) for the alpha and beta processes determined from various sources defined in the legend. The activation energy for the beta process determined from dielectric measurements is just visible under the tensile and viscoelastic data

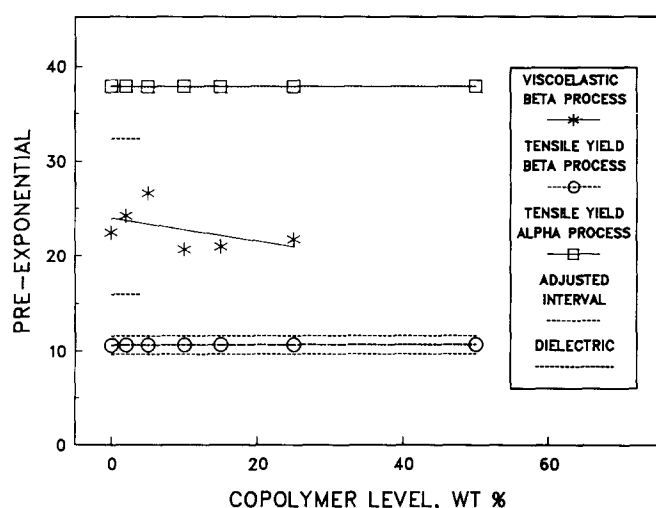


Figure 13 Pre-exponential as a function of CP-A level (in wt%) for the alpha and beta processes determined from various sources defined in the legend

of equation (5) is the pre-exponential term, often referred to as the frequency factor. Conceptually it is related to the two C_s in equation (1). The exponent of the second term on the RHS is the activation energy and is conceptually the same as the two Q_s in equation (1). Both quantities can be calculated for the viscoelastic process from the parameters C_3 and I_3 for all of the blends, and the results are given in Table 4.

Plots of the activation energies and pre-exponentials derived from viscoelastic as well as tensile yield measurements against CP-A level are given in Figures 12 and 13 respectively. In addition to the data points, confidence intervals (\pm S.D.) assuming the viscoelastic process not to depend on CP-A level and a trend line assuming the activation energy to depend on CP-A level are also included (see the legend for definitions). Only the confidence intervals for the tensile yield measurements are given in these figures. The activation energies for the viscoelastic and tensile yield studies are within two confidence intervals. There is a wide discrepancy between the pre-exponential factors calculated from the viscoelastic and tensile yield data. The pre-exponentials are related to jumping probabilities and there is no reason

to assume that they are the same for viscoelastic and tensile yield experiments. If we assume that they are proportional to one another, then equation (5) can be rewritten as:

$$f_0 \approx f_{0y} = \exp[-(\Delta E - T\Delta S)/RT]/\exp(N) \quad (7)$$

In this equation, f_{0y} is the tensile yield jumping frequency and N is a normalization constant. For the present purpose $N = 4.922$ was chosen, and the results are given in Table 4. We have plotted the mean \pm S.D. of the calculated values in Figure 13. The dielectric activation energies are also given in Figure 12 and are represented by the short broken lines. The line for the dielectric beta process is well within the error estimates, while the value for the alpha process is well below the limits.

CONCLUSIONS

Viscoelastic measurements probably offer a better method to study the effect of compositional changes on the dynamics of the glass phase because the effect of overlapping contributions due to the fact that a second component or a second process can be taken into account in these blends. This is to be expected because frequency serves as a filter to measure the responses in that specific time interval. In contrast to acting as a filter, tensile yield measurements tend to sum the responses from time $t = 0$. On the other hand the extrapolation of linear response parameters to non-linear responses such as tensile yielding must be verified experimentally. What is important here is that the linear and non-linear responses can be represented by nearly the same parameters assuming the mechanism to be molecular jumps. A shortcoming of this work is that it is limited to a single blend system. On the other hand the number of cases that exhibit this equivalence is growing.

ACKNOWLEDGEMENTS

The authors wish to express their gratitude to both G. T. Beswick and J. F. Smoyer for their helpful advice and experience with the experimental aspects of the study.

REFERENCES

- 1 Ree, T. and Eyring, H. 'Rheology' (Ed. F. R. Eirich), Academic Press, New York, 1958, Vol. II, Ch. III
- 2 Roetling, J. A. *Polymer* 1965, **6**, 311
- 3 Roetling, J. A. *Polymer* 1965, **6**, 615
- 4 Roetling, J. A. *Polymer* 1966, **7**, 303
- 5 Bauwens-Crowet, C., Bauwens, J. C. and Homes, G. *J. Polym. Sci. (A2)* 1969, **7**, 735
- 6 Havriliak, S. Jr and Shortridge, T. *J. Macromolecules* 1990, **23**, 648
- 7 Havriliak, S. Jr *J. Polym. Sci., Polym. Phys. Edn.* 1990, **28**, 1251
- 8 Havriliak, S. Jr *Colloid Polym. Sci.* 1990, **268**, 426
- 9 Havriliak, S. Jr and Shortridge, T. *J. Vinyl Tech.* 1988, **10** (3), 127
- 10 Havriliak, S. Jr and Shortridge, T. *J. Appl. Polym. Sci.* 1989, **37**, 2827
- 11 Havriliak, S. Jr and Shortridge, T. *J. Polymer* 1988, **29**, 70
- 12 Havriliak, S. Jr and Shortridge, T. *J. Polym. Eng. Sci.* 1989, **29** (12), 817
- 13 Havriliak, S. Jr and Williams, D. R. *Polymer* 1990, **31**, 115
- 14 Perchak, D., Skolnick, J. and Yaris, R. *Macromolecules* 1987, **20**, 121
- 15 Mansfield, M. L. *J. Polym. Sci., Polym. Phys. Edn.* 1983, **21** (5), 787
- 16 SAS Institute, SAS Circle, Box 8000, Carry, NC 27511, USA
- 17 Box, G. E. P., Hunter, W. G. and Hunter, J. S. 'Statistics for Experimenters, An Introduction to Design, Data Analysis and Model Building', Wiley, New York, 1978